IRAQI STATISTICIANS JOURNAL

https://isj.edu.iq/index.php/isj

ISSN: 3007-1658 (Online)

Comparative Analysis of Spline and Exponential Spline Filters for Gaussian Noise Reduction in Satellite Images: Introducing a Novel Nonlinear Filtering Approach

Mohammed Abdul Wadood Mohammed[1], Assma Ghalib Jaber[2]

[1, 2] Department of Statistics, College of Administration and Economics, University of Baghdad, Baghdad, Iraq

ARTICLE INFO

Article history:

Received	26/11/2024
Revised	26/11/2024
Accepted	14/1/2025
Available online	15/5/2025

Keywords:

Image Denoising
Image Restoration
Gaussian Noise
Spline Filter
Exponential Spline Filter

ABSTRACT

Satellite imagery often suffers from noise due to various atmospheric and sensor-related factors, which can significantly degrade image quality and hinder subsequent analysis. This article presents a comprehensive study on denoising satellite images utilizing spline interpolation and exponential spline techniques. We propose a novel nonlinear filter designed to enhance the denoising process, and we compare its performance against traditional spline-based methods. The evaluation metrics employed include the Peak Signal-to-Noise Ratio (PSNR) and Structural Similarity Index (SSIM), which are critical for assessing image quality. Our experimental results demonstrate that the proposed nonlinear filter consistently outperforms both spline interpolation and exponential spline methods, achieving superior PSNR and SSIM values. This study highlights the proposed filter's effectiveness in preserving image details while reducing noise and contributes to the ongoing advancements in remote sensing image processing techniques. The findings underscore the potential of nonlinear filtering approaches in enhancing the quality of satellite imagery for various applications.

1. Introduction

Space telescopes have revolutionized our understanding of the universe, providing scientists with high-resolution images of distant stars, galaxies, and other celestial phenomena. However, the challenge of image degradation due to noise remains a significant obstacle to fully harnessing the potential of these instruments. One of the most pervasive types of interference encountered in space telescope images is Gaussian noise, a statistical noise that disrupts the clarity of the image by adding random variations in intensity. This noise can obscure vital details, making it difficult to accurately analyze the images and extract meaningful information about the objects being observed. The presence of Gaussian noise not only affects visual quality but also undermines the precision of quantitative data derived from these images, which can hinder scientific discovery.

To address this issue, a variety of image-denoising techniques have been developed and applied in an attempt to restore image quality while preserving important structural details. Among these, the spline filter is a commonly used method due to its ability to smooth images while maintaining the integrity of edges and fine details. The spline filter works by fitting a smooth curve or surface to the noisy data, effectively reducing the fluctuations caused by noise. A related approach, the exponential spline filter, builds

* Corresponding author. E-**mail** address: mohamed.a.mohamed@coadec.uobaghdad.edu.iq

https://doi.org/10.62933/20bvef82

upon the spline filter by using an exponential weighting function, which allows for a more adaptive response to noise and helps retain sharper features in the image.

While these techniques have demonstrated success in mitigating Gaussian noise, ongoing research continues to seek improvements in image restoration methods. In this article, we examine the performance of these established filters—spline and exponential spline—and introduce a new, proposed filter designed specifically to enhance the quality of space telescope images. This proposed filter is aimed at providing a more efficient balance between noise reduction and detail preservation, which is critical when dealing with the fine structures present in astronomical images.

Through a comparative analysis of these three filters, we aim to evaluate their effectiveness in removing Gaussian noise from space telescope images. We will assess not only the visual improvements achieved by each method but also their impact on the accuracy of the data extracted from the images. By determining which filter provides the best results in terms of noise suppression and detail retention, this study seeks to contribute to the ongoing development of image-processing techniques that are essential for advancing our exploration of the universe. Ultimately, improving the quality of space telescope imagery will enable more accurate scientific observations and help unlock discoveries about the cosmos.

2. Literature Review:

In recent years, some researchers have addressed the use of these filters to reduce noise, including Oliveira et al. (2011) [24] proposed a built-in noise reduction method for reconstructed surfaces using a B-splines basis. The method was modified to accommodate different degrees of bases, ensuring smoothness levels. Simulations showed the BsART method had the smallest errors, demonstrating its superiority over post-filtered ART.

Singh et al. (2012) [33] developed an exponential B-spline interpolation kernel using Fourier approximation, achieving a high signal-to-noise ratio. The method is fast, considers polynomial spline as a special case, and uses a combination of FIR and IIR filters for fast signal decomposition and reconstruction. The interpolation function uses symmetric exponential functions of the 4th order, with complex trigonometric functions obtained for complex values.

Zhou et al. (2012) [37] applied a new multiresolution theory based on orthogonal spline to image denoising, integrating symmetry, and separating noise and image. This method improves vision quality and preserves edge information for denoised images via soft thresholding.

Fahmy's (2013) [9] study introduced a technique to enhance images by minimizing the variation function of detail coefficients in E-spline-based wavelet decomposition. This technique improves interpolated image quality and removes dependency, with examples comparing it to existing approaches.

Fahmy et al. (2013) [11] introduced a technique using E-splines for image-denoising, which uses sub-band decomposition and E-spline-based perfect reconstruction. This selective technique outperforms other methods due to its smooth transition between continuous and discrete domains.

Fahmy et al. (2013) [10] introduced a technique to minimize aliasing effects in high-frequency images using an Exponential spline scheme. They provided examples to verify the enhancement of their method.

Parveen and Tokas (2015) [29] proposed an efficient image interpolation algorithm using the cubic spline interpolation method. The algorithm enlarges the image area by inserting zeros based on zooming intensity, and estimates correct zero values.

Parsania and Virparia (2016) [28] analyzed seven nonadaptive image interpolation algorithms for real-time applications. Catmull-Rom and Mitchell-Netravali algorithms provided the best image quality and computational complexity, while Bicubic and Cubic B-spline showed less time complexity. Lanczos order 3 had the highest computational complexity.

Abdullah et al. (2018) [1] utilized the Bi-Cubic spline interpolation method for image enlargement, achieving visually bright results. Future research could combine or compare algorithms like linear interpolation, Spline, and Bi-Cubic Spline to determine their performance.

Mohammed et al. (2020) [26] focusing on the on two important criteria depending on the content including histogram and statistical criteria of the image for every color to convert images content. Several fake images are created whose content is altered. They reinforced by a number of forms, pictures, and schemes that clarify the. The steps for retrieving process have been clarified starting from statistically analysing the image and conforming it to the image formed in the database to arrange the images according to their similarity with the target one.

3. Spline Interpolation

Given a set of (n) data points (x_i, y_i), where (i = 0, 1, 2, ..., n-1), cubic spline interpolation constructs (n-1) cubic polynomials to represent the interpolated function [34]. Each cubic polynomial is defined within an interval (x_i, x_{i+1}) and passes through the data points (x_i, y_i) and (x_i, y_{i+1}) [3]. These cubic polynomials are chosen such that they are smooth (continuously differentiable) at the data points, meaning that the first and second derivatives match at the interior data points [20]. The general form of a cubic polynomial $S_i(x)$ within the interval (x_i, x_{i+1}) is given by:

$$S_i(x) = a_i + b_i(x - x_i) + c_i(x - x_i)^2 + d_i(x - x_i)^3 \quad (1)$$

where: a_i, b_i, c_i, d_i are the coefficients of the cubic polynomial $S_i(x)$ to be determined. x_i and x_{i+1} are the endpoints of the interval. To find the coefficients a_i, b_i, c_i, d_i, cubic spline interpolation imposes continuity and smoothness conditions at each data point x_i. we require that the interpolated function passes through the data point [17]. This gives:

$$Si(xi) = yi \quad (2)$$

$$Si + 1(xi) = yi \quad (3)$$

Here smoothness is ensured by requiring that the first and second derivatives of adjacent cubic polynomials match at the interior data points [6]. This leads to two additional conditions:

$$S_i'(x_{i+1}) = S_{i+1}'(x_{i+1}) \quad (4)$$

$$S_i''(x_{i+1}) = S_{i+1}''(x_{i+1}) \quad (5)$$

By combining the continuity and smoothness conditions with the general form of the cubic polynomial, we obtain a system of linear equations. Solving this system yields the coefficients (a_i, b_i, c_i, d_i) for each interval (x_i, x_{i+1}).

In image denoising, the noisy image $f(x, y)$ is treated as a set of data points (x_i, y_i), where (x) and (y) represent the spatial coordinates [1]. Cubic spline interpolation is applied to interpolate between these noisy pixel values, resulting in a smoother version of the image g (x, y) [23].

$$g(x, y) = \text{CubicSplineInterpolation}\ (f(x, y)) \quad (6)$$

The smoothness of the interpolated image helps to reduce the impact of noise while preserving important image features. This interpolated image can then be further processed using additional denoising techniques, such as Gaussian filtering to the interpolated image to reduce the noise while preserving important image features [21]. Gaussian filtering involves convolving the image with a Gaussian kernel, which is a two-dimensional Gaussian function. The Gaussian kernel is defined as [34]:

$$G(x, y) = \frac{1}{2\pi\sigma^2} e^{-\frac{x^2 - y^2}{2\sigma^2}} \quad (7)$$

where (σ) is the standard deviation of the Gaussian distribution, controlling the amount of smoothing. Larger values of (σ) result in more smoothing, while smaller values preserve finer details. The spline denoising method combines these two steps. First, the noisy image is interpolated using cubic spline interpolation to obtain a smoother version. Then, Gaussian filtering is applied to further smooth out the noise while preserving image details [7]. The resulting denoised image h (x, y) is a combination of both processes:

$$h(x,y) = \mathrm{GaussianFilter}(\mathrm{CubicSplineInterpolation}(f(x,y)) \quad (8)$$

where f (x, y) is the noisy input image, (CubicSplineInterpolation) represents the cubic spline interpolation function, and (GaussianFilter) represents the Gaussian filtering operation.

4. Exponential Spline

The exponential spline denoising method aims to smooth the noisy image while preserving edges and details [5]. The method involves applying a filter that computes a weighted average of neighboring pixel values, where the weights are determined by an exponential function [4]. The Exponential m^{th} order spline polynomial $B_m^\alpha(t)$, is constructed as m successive convolution of lower ones [19].

$$B_m^\alpha(t) = B_1^{\alpha 1}(t) * B_1^{\alpha 2}(t) * B_1^{\alpha 3}(t) \dots * B_1^{\alpha m}(t) \quad (9)$$

where $B_m^\alpha(t) = e^{\alpha t},\ 0 \le t \le 1$. The vector α can assume any positive, negative, or even complex conjugate values. This means considerable flexibility over cardinal B-spline polynomials that only use Haar functions. $B_m^\alpha(t)$ is of finite support and equals zeros at t ≤ 0 and t ≥ m. Between the knots $t = 1,2,\dots,m-1$, it is represented by polynomials of order (m-1) in t. Due to its continuity and smoothness, it is used to expand continuous signals s(t). In the discrete case, s(n) can be expressed using the convolutional relation [15].

$$s(n) = \sum_k c(k)\, B_m^\alpha(n-k) \quad (10)$$

The c_k coefficients are obtained using the concept of inverse filtering described in, an alternate approach given to determine these coefficients as the solution of the linear system

$$s = Bc \quad (11)$$

$$s = [s_1\ s_2\ s_3 \dots s_N]^t \quad (12)$$

$$c = [c_1\ c_2\ c_3 \dots c_N]^t \quad (13)$$

$$B = \begin{bmatrix} B_m^\alpha\left(\frac{m}{2}\right) & B_m^\alpha\left(\frac{m}{2}-1\right) & & 0 \\ B_m^\alpha\left(\frac{m}{2}+1\right) & B_m^\alpha\left(\frac{m}{2}\right) & & \\ & & B_m^\alpha\left(\frac{m}{2}\right) & B_m^\alpha\left(\frac{m}{2}-1\right) \\ 0 & & B_m^\alpha\left(\frac{m}{2}+1\right) & B_m^\alpha(t) \end{bmatrix} \quad (14)$$

The solution of this system results in exact interpolation for any specified α. The L-interpolated E-spline polynomial is defined by inserting (L-1) equal-spaced points between every two knots of the E-spline polynomial, i.e $\left\{B_m^{\alpha,L}(t) = B_m^\alpha\left(\frac{t}{L}\right)\right\}$. the complete perfect reconstruction E-splines wavelet family has been constructed for any arbitrary choice of α. First, the E-spline 2-scale relation is defined by [22].

$$B_m^\alpha(t) = \sum_{k=-m}^{m} p(k) B_m^\alpha(2t-k) \quad (15)$$

$$p(z) = \frac{1}{2}\sum_{k=-m}^{m} p(k) z^{-k} \quad (16)$$

$$z = e^{j\frac{w}{2}} \quad (17)$$

has been determined for any arbitrary n α. were, the wavelet E–spline function $U_m^\alpha(t)$, satisfying the orthogonality relation:

$$\int_{-m}^{m} U_m^\alpha(t) B_m^\alpha(t-1)\, dt = 0 \quad (18)$$

$$U_m^\alpha(t) = \sum_{k=-m}^{m} q(k) B_m^\alpha(2t-k) \quad (19)$$

$$Q(z) = \frac{1}{2}\sum_{k=-m}^{m} q(k) z^{-k} \quad (20)$$

Moreover, the Exponential dual scaling A(z) and wavelet E-spline functions B(z), have been constructed for any arbitrary α . Finally, it has been shown that the following perfect construction (PR) relation is satisfied [39].

$$p(z)A(z^{-1}) + Q(z)B(z^{-1}) = 1 \quad (21)$$

$$p(-z)A(z^{-1}) + Q(-z)B(z^{-1}) = 0 \quad (22)$$

to use the E-spline wavelet family discussed above in denoising noisy images. Wavelet decomposition amounts to representing signals by few nonzero coefficients. In case of a noisy data x, that represents a signal f corrupted with uncorrelated zero mean noise w, i.e. $x = f + w$, these coefficients are given by [14].

$$\langle x, U_{l,m}\rangle = \langle f, U_{l,m}\rangle + \langle w, U_{l,m}\rangle \quad (23)$$

Where $\langle . \rangle$ is the inner product and $U_{j,m}$ represents the j^{th} scale wavelet basis used. As physical signals like speech and images are nominally treated as baseband signals, the wavelet coefficients at fine scales, are mainly due to noise and have to be thresholded, for signals corrupted with zero mean Gaussian noise, the threshold level is [2].

$$T = \sigma \log (\sqrt{2N}) \quad (24)$$

N is the noisy signal length, while σ^2 is the associated noise variance. The variance is estimated from the median M of the noisy signal [40], as

$$\sigma = \frac{E(M)}{0.6745} \quad (25)$$

5. Proposed Filter:

The proposed filter converts the image from RGB to YUV color space as step one, where the (Y, U, V) color space is a color representation used in digital image and video processing. It separates the luminance (brightness) information from the chrominance (color) information in an image [23]. then in step two, we split the image channels to extract the noisy (Y) channel and apply a bandwidth selection method on this (Y) channel, where the bandwidth selection, or smoothing parameter (h) is a crucial step in nonparametric estimation techniques, particularly kernel density estimation and kernel regression [16]. It involves determining an appropriate bandwidth parameter (h) that controls the smoothing or blurring effect of the kernel function [30].

Nonparametric estimation aims to estimate an underlying probability density function or regression function from a given set of data points. The kernel function is a smooth, symmetric function cantered at each data point, and the bandwidth determines the width of this kernel function [31]. The choice of bandwidth significantly influences the quality and accuracy of the estimated function. If the bandwidth is too large, the estimate may become overly smooth and fail to capture important features or structures in the image. On the other hand, if the bandwidth is too small, the estimate may exhibit excessive noise and reflect the specific characteristics of individual data points rather than the underlying pattern.

Cross-validation (CV) is a method that offers a criterion for optimality that works as an empirical analog of the (MISE) and so it allows us to estimate (h). There are three types of (CV), Least Squares Cross-Validation (LSCV), also called unbiased (UCV), involves the (ISE) [12].

$$ISE_h = \int_{-\infty}^{\infty} (\hat{f}_h(x) - f(x))^2 dx \quad (26)$$

Where (f(x)) and ($\hat{f}_h(x)$) is the density and density estimator, which leads to

$$\hat{h}_{LSCV} = \text{argmin } (LSCV_h) \quad (27)$$

Biased Cross-Validation (BCV), where it attempts to directly minimize the (AMISE). This requires an estimation of the unknown R(f"), which requires selecting another bandwidth [18].

$$AMISE = \frac{K}{nh} + \frac{K_2^2 \, R(f'')}{nh} \quad (28)$$

By replacing the unknown values in the $\{R(f'')\}$ term with the estimate $\{\tilde{R}(f'')\}$, we obtain the $\{BCV_h\}$ estimator:

$$BCV_h = \frac{K}{nh} + \frac{K_2^2}{nh}\left(R\left(\hat{f}_h''\right) - \frac{R(K'')}{nh^5}\right) \quad (29)$$

$$\therefore \hat{h}_{BCV} = \text{argmin } CV(h) \quad (30)$$

Maximum Likelihood Cross Validation (MLCV). The rationale behind this method is to estimate the log-likelihood of the density at observation (x_i) based on all observations except (x_i). Averaging this log-likelihood over all observations results in the following (MLCV) score [32].

$$\hat{h}_{MLCV} = \text{argmin } CV(h) \quad (31)$$

MLCV seeks to test the hypothesis:

$$\left.\begin{array}{l} H_0: \hat{f}_x = f_x \\ H_0: \hat{f}_x \neq f_x \end{array}\right\} \quad (32)$$

The next step, bandwidth parameters (h) for the (Y) channel that we get by (CV), use it for density estimation, where the Kernel density estimation (KDE) is a non-parametric method used to estimate the probability density function (PDF) of a random variable based on a set of observed data points [10]. KDE works by placing a kernel (a smooth, symmetric, and non-negative function) on each data point and summing up these kernels to obtain the estimated PDF [32]. The estimated density at any point x is formulated as [8].

$$\hat{f}_h(x) = \frac{1}{n}\sum_{i=1}^{n} K\left(\frac{x - X(i)}{h}\right) \tag{33}$$

where x(i) is a neighboring point to (x), (n) is the number of neighbors, K (·) is the kernel function, and (h) is the bandwidth. The kernel function can be considered a weighting factor that gives a larger value when x(i) is close to (x). This density estimation will reconstruct the (Y) channel then in the next step, we apply the denoising method to get the denoised (Y) channel which we use to rebuild the new denoised image in the final step. For the denoising task, there are several denoising methods or filters.

Total Variation (TV) is a technique used for image denoising and restoration. TV method effectively reduces noise while preserving edges and important image structures by minimizing the total variation of an image, which is a measure of the total amount of variation or changes between neighboring pixels [36]. For the image denoising task, TV assumes that the noisy image y(n) is of the form

$$y_n = x_n + w_n \qquad n = 0, \dots, N-1 \tag{34}$$

where x(n) is a (approximately) piecewise constant signal and w(n) is white Gaussian noise. (TV) estimates the image x(n) by solving the optimization problem

$$\operatorname{argmin}_x = \left\{F_x = \frac{1}{2}\sum_{n=0}^{N-1}|y_n - x_n|^2 + \lambda\sum_{n=1}^{N-1}\left|x_n - x_{(n-1)}\right|\right\} \tag{35}$$

The regularization parameter $\lambda > 0$ controls the degree of smoothing. Increasing λ gives more weight to the second term which measures the fluctuation of the signal x(n) [38]. the TV denoising in equation (2) can be written compactly as:

$$\operatorname{argmin}_x = \left\{F_x = \frac{1}{2}\|y - x\|_2^2 + \lambda\|D_x\|_1\right\} \tag{36}$$

The N-point signal x is represented by the vector [13]:

$$X = [x_0, x_1, \dots, x_{N-1}]^T \tag{37}$$

Classical ℓ_1 TV computed independently on each color component [25].

$$\|X\|_1 = \sum\|X_k\|_1 \quad (p = 1, q = 1) \tag{38}$$

ℓ_2 TV computes the Euclidean norm of the vector

$$\|X\|_2 = \left(\sum_k X_k^2\right)^{\frac{1}{2}} (p = 2, q = 1) \tag{39}$$

Squared $\ell 2$ TV computes the squared Euclidean norm of the vector [27].

$$\|X\|_2 = \left(\sum_k X_k^2\right) (p = 2, q = 2) \tag{40}$$

The matrix D is defined as [25]

$$D = \begin{bmatrix} -1 & 1 & \cdots & 0 & \\ \vdots & & \ddots & \vdots & \\ 0 & & \cdots & -1 & 1 \end{bmatrix} \tag{41}$$

The first-order difference of an N-point image x is given by D_x where D is of size $(N-1) \times N$. Note, for later, that DD^T is a tridiagonal matrix of the form:

$$D = \begin{bmatrix} 2 & -1 & & \cdots & 0 & \\ -1 & 2 & -1 & & & \\ \vdots & & & \ddots & \vdots & \\ 0 & & & \cdots -1 & 2 & -1 \\ & & & -1 & & 2 \end{bmatrix} \tag{42}$$

The total variation of the N-point image x(n) is given by

$$TV(x) = \|D_x\|_1 = \sum_{n=1}^{N-1}\left|x_n - x_{(n-1)}\right| \tag{43}$$

The main advantage of the TV formulation is the ability to preserve edges in the image due to the piecewise smooth regularization property of the TV norm.

Finally, after we get the new denoised Y channel, we can reconstruct the denoised image by merging the new Y channel with the U and

V channels replace the denoised Y channel with the noise Y channel in the image.

6. Results and discussion

To compare the results of the filters used, we relied on two quality measurement criteria, The Peak Signal Noise Ratio (PSNR) which is the ratio of the maximum image values to the magnitude of noise affecting the image

$$\mathrm{PSNR}_{(X,Y)} = 10 * \log_{10} \frac{(\mathrm{MAX}^2_{\mathrm{pixels}})}{(\mathrm{MSE})} \quad (41)$$

Where the original image (X) and the resulting image (Y) are compared using the Max brightness value (255) and the mean square error (MSE) between the two images.

And the SSIM index measures structural similarity between two images, with perfect quality indicating the quality of the other image being compared.

$$\mathrm{SSIM}_{(X,Y)} = \frac{(2\mu_x\mu_y + C_1)(2\sigma_{xy} + C_2)}{(\mu_x^2 + \mu_y^2 + C_1)(\sigma_x^2 + \sigma_y^2 + C_2)} \quad (42)$$

The experiment was carried out by adding AWGN with zero mean and 0.75 variance to the approved image as shown in Figure 1, which is a dumbbell nebula, Considering the significance of these images, we should work to eliminate any noise that may have been introduced during the transmission and acquisition process. So, in this experiment, we added different percentages of Gaussian noise to the adopted image and then applied the adopted filters, the code of these filters is written using MATLAB.

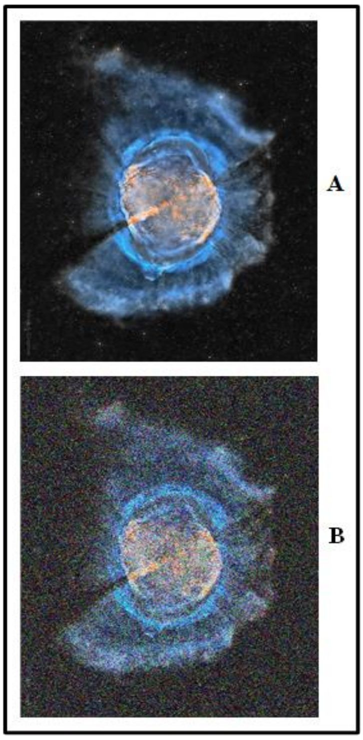

Figure 1: dumbbell nebula (**A**) Clean Image, (**B**) Noisy Image.

The results indicate that the proposed filter performs best in terms of both PSNR and SSIM when there is a noise density of 0.01 where it is given the value 38.70 PSNR, and 0.96 SSIM respectively, while the Spline filter ranks second with 31.22 PSNR and 0.91 SSIM. According to measurements, E spline filters have the values 30.12 PSNR and 0.90 SSIM, respectively. Figure 2 displays the images that have been restored.

Table 1: PSNR and SSIM Values for The Restored Images for Each Filter

Filters	Image Quality Measurements	
	PSNR	SSIM
Proposed	38.70	0.96
Spline	31.22	0.91
E-Spline	30.12	0.90

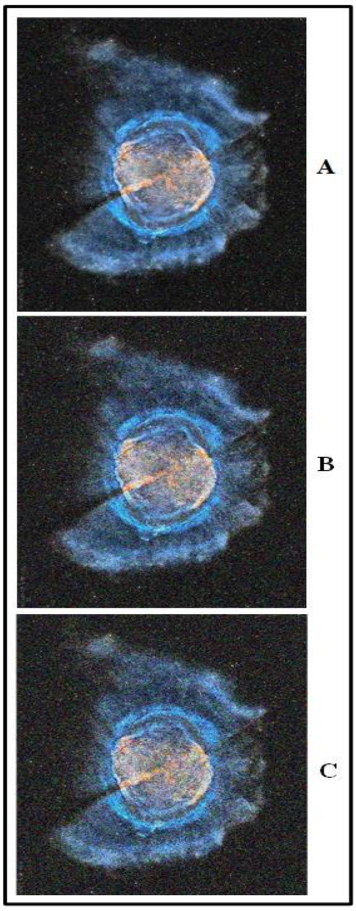

FIGURE 2. Restored Image by (**A**) Proposed Filter, (**B**) Spline Filter, (**C**) E-Spline Filter.

The mechanism used by the proposed method to analyze the image, which was represented by a series of stages, is what accounts for its superiority. First, an appropriate bandwidth parameter was extracted using a plug-in method designed to minimize errors. The Gaussian density function was then estimated using this parameter by calculating the mean and variance of the noise contained in the image. Finally, a useful denoising method is to divide the image using thresholding.

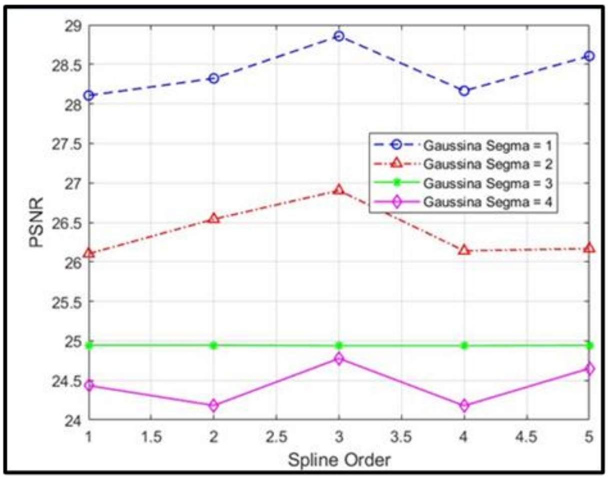

FIGURE 3. Image Quality in Different Gaussian Sigma and Spline Order Values.

Spline filter algorithm depends on Spline Order, Spline Spacing, and Gaussian Sigma to achieve the denoising process. To choose the best parameters that minimize noise while preserving essential details, we experiment with different combinations of these parameters until we find the best balance between noise reduction and detail preservation. We experiment with Spline Order with the values (1, 2, 3, 4, 5), Spline Spacing with the values (1, 2, 3, 4, 5), and Gaussian sigma (1, 2, 3, 4).

The exponential Spline algorithm depends on two parameters lambda (λ) and Sigma (σ). (λ) controls the strength of smoothing in the filter. Were a higher value of (λ) will result in stronger smoothing, while a lower value will have less smoothing effect. We start with a moderate value, such as ($\lambda = 100$). This is a common starting point for many denoising tasks. And then adjust lambda based on visual inspection of the denoised image.

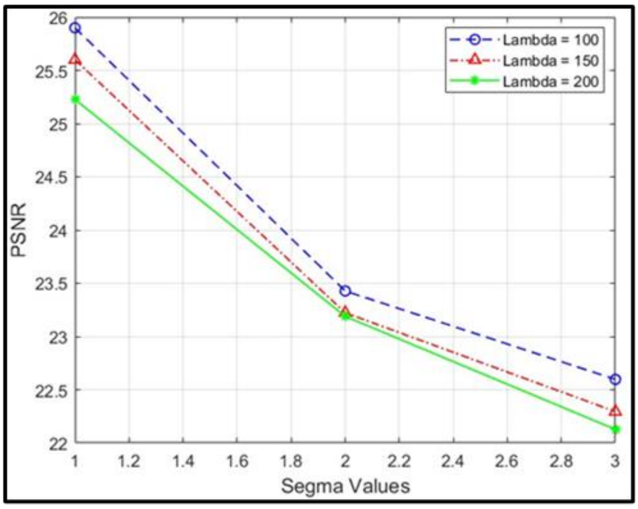

FIGURE 4. Image Quality in Different Lambda and Sigma Values.

7. Conclusions

The study presents a new method for denoising Gaussian noise in satellite images using YUV color space techniques. The method converts the noisy image to the YUV color space, focuses on the noisy Y channel, and estimates its density function using cross-validation. This method significantly outperforms traditional denoising methods in terms of visual quality and quantitative metrics. It preserves image details while reducing artifacts, making it suitable for satellite image processing applications.

References

1. Abdul Wadood, M., & Ghalib, A. (2024). Gaussian Denoising for the First Image from The James Webb Space Telescope “Carina Nebula” using Non-Linear Filters. *Journal of Economics and Administrative Sciences, 30*(143), 420-434.
2. Abdullah, D., Fajriana, F., Maryana, M., Rosnita, L., Putera, A., Siahaan, U., Hadikurniawati, W. (2018). The application of an interpolation image is done using a bi-cubic algorithm. *IOP Conf. Series: Journal of Physics: Conf. Series, 1114*, 1-7. doi:https://doiorg/10.1088/1742-6596/1114/1/012066
3. Anne, T., & Neri, M. (n.d.). A Heuristic Spline Interpolation Method on Signal Denoising.
4. Averbuch, A. Z., Neittaanmäki, P., & Zheludev, V. (2016). *Spline and Spline Wavelet Methods with Applications to Signal and Image Processing Volume II: Non-Periodic Splines.* New York: Springer Science and Business Media. doi:https://doi.org/10.1007/978-3-319-22303-2
5. Averbuch, A., Neittaanmki, P., Shabat, G., & Zhelludev, V. (2016). Fast Computation By Subdivision Of Multidimensional Splines And Their Applications. *1*(3), 309-341. Retrieved from http://www.ybook.co.jp/online2/oppafa/vol1/p309.html
6. Averbuch, A., Zheludev, V., Neittaanmaki, P., & Kore, J. (2010). Block-based deconvolution algorithm using spline wavelet packets. *Journal of Mathematical Imaging and Vision, 38*, 197–225. doi:https://doi.org/10.1007/s10851-010-0224-4
7. Basco-Uy, T. A., & Neri, M. C. (2020, 8 1). A Heuristic Spline Interpolation Method on Signal Denoising. *15*(1), 1-11.
8. Cassanya, V., Barrutia, M., & Unser. (2007). Locally adaptive smoothing method based on B-splines based on B-splines. 1-7.
9. Chac´on, J., & Duong, T. (2019). Multivariate plug-in bandwidth selection with unconstrained pilot bandwidth matrices. *International Journal of Development Research, 7*(9), 15048–15053. doi:https://doi.org/10.1007/s11749-009-0168-4
10. Fahmy, G. (2013). Image Super-Resolution and Enhancement Using E-spline. *Journal of Communication and Computer, 10*, 1497-1501. doi:http://dx.doi.org/10.1109/ISSPIT.2013.6781890
11. Fahmy, M. F., Fahm, G., & Fahm, O. M. (n.d.). E-spline Based Image Interpolators. *IEEE International Symposium on Signal Processing and Information Technology (ISSPIT), 32*, 61-68. doi:https://doi.org/10.1109/isspit.2014.7300564
12. Fahmy, M., Fahmy, G., & Alkanhal, T. (2013). E-Spline In Image De-Noising Applications. *30th National Radio Science Conference, 7*, 274-280. doi:https://doi.org/10.1109/nrsc.2013.6587924
13. Florence, K., Aggrey, A., & Leonard, K. (2018, 5 24). Efficiency of various Bandwidth Selection Methods across Different Kernels.

IOSR Journal of Mathematics (IOSR-JM), 15(3), 55-62. doi:https://doi.org/10.9790/5728-1503015562

14. Ghalib, A., & Abdul Wadood, M. (2020). Using multidimensional scaling technique in image dimension reduction for satellite image. *Periodicals of Engineering and Natural Sciences, 8*(1), p.447-454.

15. Getreuer, P. (2012). Rudin–Osher–Fatemi Total Variation Denoising using Split Bregman. *Image Processing On Line, 2*, 74–95. doi:https://doi.org/10.5201/ipol.2012.g-tvd

16. Hong, Q., Hong, Q., Messi, L., & Wang, J. (2019). Galerkin method with splines for total variation minimization. *Journal of Algorithms & Computational Technology, 13*, 1-16. doi:http://dx.doi.org/10.1177/1748301819833046

17. Horiuchi, Y. (n.d.). Reducing Image Noise Using Spline Smoothing. 1-4.

18. Horova, I., Kolacek, J., Zelinka, J., & Vopatova, K. (2008, 12). Bandwidth choice for kernel density estimates. 1-10. Retrieved from https://link.springer.com/article/10.1007/s10182-013-0216-y

19. Islam, T., & Righetti, R. (2020). A Spline Interpolation–based Data Reconstruction Technique for Estimating Strain Time Constant in Ultrasound Poroelastography. *Electrical Engineering and Systems Science, 42*(1), 5-14. doi:https://us.sagepub.com/en-us/journals-permissions

20. Jones, M. C., Marron, J. S., & Sheather, S. J. (1996, 3). A Brief Survey of Bandwidth Selection for Density Estimation. *Journal of the American Statistical Association, 91*(433), 401-407. Retrieved from https://www.jstor.org/stable/pdf/2291420.pdf

21. Kawasakia, T., Jayaraman, P., Shida, K., Zheng, J., & Maekawa, T. (2018). An Image Processing Approach to Feature-Preserving B-Spline Surface Fairing. 1-14.

22. Lakshmi, M., Murthy, S., & Rao, N. (2017). A Novel Algorithm for Impulse Noise Removal using B-Splines for Finger Print Forensic Images. *International Journal of Applied Engineering Research, 12*(1), 127-131.

23. Lee, J. C., Li, J., Musco, C., Phillips, J., & Tai, W. M. (2021). Finding an Approximate Mode of a Kernel Density Estimate. *29th Annual European Symposium on Algorithms (ESA 2021)*(61), 1-19.

24. Mccartixn, B. J. (1991). Theory Of Exponential Splines. *Journal Of Approximation Theory*, 1-23.

25. Mohammed, A., Jamil, B., Ali, F. (2020). Bootstrap technique for image detection. *Periodicals of Engineering and Natural Sciences*. *8*(3), 1280-1287. https://api.semanticscholar.org/CorpusID:221757811.

26. Mohammed, F., Fahmy, G., & Fahmy, O. (2011, 7). B-spline wavelets for signal denoising and image compression. *Signal Image and Video Processing, 5*, 141–153. doi:https://doi.org/10.1007/s11760-009-0148-x

27. Oliveira, E. F., Melo, S. B., Dantas, C. C., Mota, Í. V., & Lira, M. (2011, 10 24). Tomographic Reconstruction With B-Splines Surfaces. *2011 International Nuclear Atlantic Conference - INAC 2011*, 1-14.

28. Ortelli, F., & van de Geer, S. (2020). Adaptive Rates for Total Variation Image Denoising. *Journal of Machine Learning Research, 21*, 1-38.

29. Pana, H., Wena, Y.-W., & Zhu, H.-M. (2019, 11 23). A regularization parameter selection model for total variation-based image noise removal. *Applied Mathematical Modelling, 68*, 353-376. doi:https://doi.org/10.1016/j.apm.2018.11.032

30. Parsania, P. S., & Virparia, P. V. (2016, 1). A Comparative Analysis of Image Interpolation Algorithms. *International Journal of Advanced Research in Computer and Communication Engineering, 5*(1), 29-34. doi:https://doi.org/10.17148/IJARCCE.2016.5107

31. Parveen, S., & Tokas, R. (2015). Faster Image Zooming using the Cubic Spline Interpolation Method. *International Journal on Recent and Innovation Trends in Computing and Communication, 3*(1), 22 - 26. doi:https://doi.org/10.17762/ijritcc2321-8169.150106

32. Rothfuss, J., Ferreira, F., Walther, S., & Ulrich, M. (2019, 4 3). Conditional Density Estimation with Neural Networks: Best Practices and Benchmarks. 1-36. Retrieved from https://arxiv.org/abs/1903.00954

33. Salgado-Ugarte, I. H., & Perez-Hernandez, M. A. (2003). Exploring the use of variable bandwidth kernel density estimators. *The Stata Journal, 3*(2), 133-137. Retrieved from https://www.stata-journal.com/abstracts/st0036.pdf

34. Sharma, A., Lall, U., & Tarboton, D. G. (1998). Kernel bandwidth selection for a first-order nonparametric streamflow simulation model. *Statistic Hydrology and Hydraulics, 12,* 33-52. Retrieved from https://link.springer.com/article/10.1007/s004770050008

35. Singh, R. B., Jain, A., & Lipton, M. (2012, 12). Image Enhancement Method using E-spline. *International Journal of Emerging Trends & Technology in Computer Science (IJETTCS), 1*(4), 35-43.

36. Takeda, H., Farsiu, S., & Milanfar, P. (2007, 2). Kernel Regression for Image Processing and Reconstruction. *IEEE Transactions On Image Processing, 16*(2), 349-366. doi:https://doi.org/10.1109/TIP.2006.888330

37. Xu, G., Ling, R., Deng, L., Wu, Q., & Ma, W. (2020). Image Interpolation via Gaussian-Sinc Interpolators with Partition of Unity. *Computers, Materials & Continua, 62*(1), 309-319.

38. Zeng, X., & Li, S. (2013). An efficient adaptive total variation regularization for image denoising. *Conference: Image and Graphics (ICIG), 7*, 1-6. doi:https://doi.org/10.1109/ICIG.2013.17

39. Zhou, K., Zheng, L., & Lin, F. (2012). Image Denoising Using Orthogonal Spline. *Physics Procedia; 2012 International Conference on Medical Physics and Biomedical Engineering, 33*, 798 – 803. doi:https://doi.org/10.1016/j.phpro.2012.05.137

40. Zhu, J., Li, K., & Hao, B. (2019, 5 6). Image Restoration by Second-Order Total Generalized Variation and Wavelet Frame Regularization. *Complexity*, 1-17. doi:https://doi.org/10.1155/2019/3650128